



Research article

Li₄GeO₄-Li₂CaGeO₄ phase equilibria and Li_{2+*x*}Ca_{1-*x*}GeO₄ solid solutionsV. Nikolov^{a,*}, R. Nikolova^a, N. Petrova^a, P. Tzvetkov^b, I. Koseva^b^a Institute of Mineralogy and Crystallography, Bulgarian Academy of Sciences, 1113, Sofia, Bulgaria^b Institute of General and Inorganic Chemistry, Bulgarian Academy of Sciences, 1113, Sofia, Bulgaria

ARTICLE INFO

Keywords:

- A. oxide materials
- A. inorganic materials
- B. solid state reactions
- C. crystal structure
- C. phase diagrams
- D. X-ray diffraction

ABSTRACT

Detailed studies of the Li₄GeO₄-Li₂CaGeO₄ system by solid-phase syntheses of various compositions from pure Li₄GeO₄ to pure Li₂CaGeO₄ in the temperature range from 25 to 1125 °C is investigated for a first time. Solid state synthesis powders are characterized by X-ray and DSC/TG methods. Concentration and temperature two-phase regions of Li₄GeO₄ and Li₂CaGeO₄ as well as two-phase regions of Li₂CaGeO₄ and Li_{2+2*x*}Ca_{1-*x*}GeO₄ are established. Region of pure Li_{2+2*x*}Ca_{1-*x*}GeO₄ solid solution are detected too and its structure is investigated. Being structural analog to Li_{2+2*x*}Zn_{1-*x*}GeO₄ and Li_{2+2*x*}Mg_{1-*x*}GeO₄, Li_{2+2*x*}Ca_{1-*x*}GeO₄ has own specific local environment of the metal ions. The obtained results are compared with those for Li₄GeO₄-Li₂ZnGeO₄ system and for Li_{2+2*x*}Zn_{1-*x*}GeO₄ solid solution. The differences of the phase diagrams and structural features of the solid solutions are discussed.

1. Introduction

Germanate compounds are widely used for various applications such as dielectric ceramics, optics, optoelectronics and lasers. Most of them are isostructural to the corresponding silicate compounds, but compared to the latter, they have lower melting temperatures, which facilitate their synthesis as powders, glasses, glass-ceramics or single crystals. Among the widely used germanates are those from the systems Zn₂GeO₄-Li₄GeO₄, Mg₂GeO₄-Li₄GeO₄ and Ca₂GeO₄-Li₄GeO₄.

Mg₂GeO₄ and Zn₂GeO₄, for example, have been tested as dielectric ceramics [1,2] as well as phosphors when doped with transition ions or rare earth ions for different emission in the visible region [3,4].

The intermediate compounds from these systems Li₂ZnGeO₄, Li₂MgGeO₄ and Li₂CaGeO₄ have been tested also as dielectric ceramics [5,6] and phosphors [7–11]. Another promising application of these intermediates is for solid-state laser media doped with Cr⁴⁺ possessing a wide spectrum of radiation in the near infrared region (1.1–1.6 μm) [12,13]. An advantage of these compounds for this application is the fact that all metal ions in their structure (Li, Zn, Mg, Ca, Ge) are in a tetrahedral environment, guaranteeing doping with an active Cr⁴⁺ ion, replacing Ge⁴⁺ and preventing doping with the unwanted in this case of application Cr³⁺ (as the Cr³⁺ prefers an octahedral environment) [14]. An additional advantage is that the lifetime of the active ion Cr⁴⁺ in these laser media is significantly longer than that of the solid-state media Mg₂SiO₄ and Y₃Al₅O₁₂ widely used for lasers in the near infrared region up to now [15].

A particularly important area of the Me₂GeO₄-Li₄GeO₄ systems is the Li₂MeGeO₄-Li₄GeO₄ subsystems (where Me is Zn, Mg or Ca). After replacing of Me by Li in these subsystems, solid solutions with the general formula Li_{2+2*x*}Me_{1-*x*}GeO₄ crystallize. These solid

* Corresponding author.

E-mail address: velin_nikolov@yahoo.com (V. Nikolov).

solutions are isostructural to the orthorhombic γ - Li_3PO_4 and to the high-temperature modifications of $\text{Li}_2\text{ZnGeO}_4$ and $\text{Li}_2\text{MgGeO}_4$. Due to their specific structure, some of the Li ions are particularly mobile, which predetermines the high ionic conductivity of these solid solutions. The solutions are known as LISICON (lithium superionic conductors). Apart from their high conductivity, some of these solutions (according to the available data) are thermodynamically stable, i.e. unlike of $\text{Li}_2\text{MeGeO}_4$, they do not show polymorphic transitions, which offers opportunities for single crystal growth (e.g. for solid-state lasers application).

The successful synthesis of germanate compounds and understanding the mechanism of ionic conductivity, as well as the features of excitation and emission after doping for one or another application, requires knowledge of the concentration and temperature regions of crystallization into the systems $\text{Li}_2\text{MeGeO}_4$ - Li_4GeO_4 including these of the $\text{Li}_{2+2x}\text{Me}_{1-x}\text{GeO}_4$ solid solutions, as well as the crystal structure features of the last upon changes in the Li/Me ratio. But in fact, only the $\text{Li}_2\text{ZnGeO}_4$ - Li_4GeO_4 and $\text{Li}_{2+2x}\text{Zn}_{1-x}\text{GeO}_4$ solid solutions have been studied in details [16–20]. For $\text{Li}_2\text{MgGeO}_4$ - Li_4GeO_4 and especially for $\text{Li}_2\text{CaGeO}_4$ - Li_4GeO_4 available data are scarce [21–23].

$\text{Li}_2\text{CaGeO}_4$ - Li_4GeO_4 system was not investigated and no data about the concentration and temperature regions of the crystallizing phases including $\text{Li}_{2+2x}\text{Ca}_{1-x}\text{GeO}_4$. $\text{Li}_2\text{CaGeO}_4$ was established to be tetragonal and isostructural to $\text{Li}_2\text{CaSiO}_4$ [21], but in accordance to Monaye et al. [22], $\text{Li}_2\text{CaGeO}_4$ is orthorhombic, being synthesized at the temperature between 1100 and 1300 °C. For $\text{Li}_{2+2x}\text{Ca}_{1-x}\text{GeO}_4$ was published only that these solid solutions consist at 900 °C for x from 0.65 to 0.95, no consist below 635 °C and possess low value of ion conductivity [23].

The main aim of our work was to investigate the $\text{Li}_2\text{CaGeO}_4$ - Li_4GeO_4 system, establishing the concentration and temperature regions of the crystallizing phases including that of $\text{Li}_{2+2x}\text{Ca}_{1-x}\text{GeO}_4$ and to investigate the structure of these solid solutions.

2. Experiment

The following starting reagents were used for the research: Li_2CO_3 (99.9%), CaCO_3 (99.9%) and GeO_4 (99.99%). The reagents were preliminary preheated at 200 °C to a constant weight. The percentage of moisture in the starting reagents was determined by the difference in weight before and after heat treatment. Li_2CO_3 and CaCO_3 were found to contain 1.2% and 0.3% moisture, respectively, and GeO_4 did not change its weight. The phase diagram was mainly investigated by synthesizing and analyzing samples with different initial compositions between $\text{Li}_2\text{CaGeO}_4$ and Li_4GeO_4 describing with a total formula $\text{Li}_{2+2x}\text{Ca}_{1-x}\text{GeO}_4$, where x was changed with a step of 0.1 (x = 0, 0.1, 0.2, 0.3, 0.4, 0.5, 0.6, 0.7, 0.8, 0.9 and 1.0), i.e. samples with chemical compositions $\text{Li}_2\text{CaGeO}_4$, $\text{Li}_{2.2}\text{Ca}_{0.9}\text{GeO}_4$, $\text{Li}_{2.4}\text{Ca}_{0.8}\text{GeO}_4$, $\text{Li}_{2.6}\text{Ca}_{0.7}\text{GeO}_4$, $\text{Li}_{2.8}\text{Ca}_{0.6}\text{GeO}_4$, $\text{Li}_{3.0}\text{Ca}_{0.5}\text{GeO}_4$, $\text{Li}_{3.2}\text{Ca}_{0.4}\text{GeO}_4$, $\text{Li}_{3.4}\text{Ca}_{0.3}\text{GeO}_4$, $\text{Li}_{3.6}\text{Ca}_{0.2}\text{GeO}_4$, $\text{Li}_{3.8}\text{Ca}_{0.1}\text{GeO}_4$ and Li_4GeO_4 were investigated. The starting reagents were mixed in the desired quantitative ratio and stirred for homogenization in an agate mortar. The prepared mixtures, weighing about 2 g, were loaded into a platinum crucible for subsequent solid-phase synthesis. The syntheses were carried out by heating the samples with rate 200 °C/h to 700 °C, hold at this temperature for 3 h, stirred again, heat to 900 °C and hold at this temperature for 6 h. The synthesis regime described was chosen based on preliminary studies to avoid evaporation of components during synthesis and reaching full synthesis without further change in the phase composition (Li_2O partially evaporates during faster heating, and the synthesis down 900 °C is not completed). To study the changes in the obtained phase depending on the temperature, the samples with different composition, synthesized at 900 °C were additionally treated at 700 °C, 500 °C, 300 °C and 100 °C for 12, 24, 48, and 72 h. The specified treatment times were also determined by preliminary tests, guaranteeing reaching unchanged phase composition of the samples. Another part of these samples was treated at temperatures above 900 °C to establish the temperature of complete or partial melting (congruent or incongruent melting). All samples were rapidly cooled to room temperature after synthesis (in about 10 min) by direct removal from the furnace.

Except to the described basic studies, additional studies of compositions at other values of x, other temperatures as well as at other cooling regimes of treatment times were carried out to clarify the phase diagram. These additional studies will be described in the Result and Discussion part.

The syntheses were carried out in a resistive Kanthal furnace equipped with a Eurotherm 2704 programmer controller, guaranteeing temperature maintenance with an accuracy of 0.1 °C and different rates of controlled temperature change.

The XRD patterns were collected at room temperature in the range 5–80° 2 θ on a Bruker D8 Advance diffractometer using CuK α radiation and LynxEye position sensitive detector. The identification of crystalline phases and semi-quantitative analysis was performed by using ICDD PDF-2 Database (release 2021) and Bruker Diffrac.Eva V.4.0 program.

To study of the $\text{Li}_{2+2x}\text{Ca}_{1-x}\text{GeO}_4$ structure an X-ray single crystal diffractometer Bruker D8 Venture was used. The data collection and data reduction were performed by CrysAlisPro [24]. The crystal structure was solved ab initio with SHELXT [25] and refined by the full-matrix least-squares method of F2 with ShelXL [26] programs.

The differential scanning calorimetry (DSC) and thermogravimetry (TG) were carried out on an analyzer Setsys Evolution 2400, SETARAM. Part of the samples were investigated at the following conditions: heating from 20 to 800 °C and then cooling from 800 to 50 °C with a heating/cooling rate of 10 °C min⁻¹ in a static air atmosphere. Sample mass of 10–12 mg was plated in a corundum crucible. Other empty corundum crucible was used as a reference. A calibration run with empty crucibles was applied for all experiments to base line slope correction of both DSC and TG signal. Other samples were heated from 20 to 800 °C with a heating rate of 10 °C min⁻¹ in a static air atmosphere. In this case, to clarify the nature of the established changes during heating a simultaneous analysis of the evolved gases was provided using an OmniStar mass spectroscopy (MS) equipment connected to the DSC-TG apparatus. The intensities related to the m/z values of CO₂ (44) and H₂O (18) were examined. Specialized CALISTO thermal analysis software for conducting the experiments and processing the results was used.

3. Result and discussion

The experimentally established phase equilibria in the $\text{Li}_4\text{GeO}_4\text{-Li}_2\text{CaGeO}_4$ system for compositions from pure Li_4GeO_4 to pure $\text{Li}_2\text{CaGeO}_4$ for temperature range from 25 to 1125 °C are presented in Fig. 1.

It was detected that the diagram includes the following phase regions:

In the temperature range from 1000 to 1125 °C, for values of x from 0 to 0.65 into the starting chemical composition $\text{Li}_{2+2x}\text{Ca}_{1-x}\text{GeO}_4$ (between lines a and b in Fig. 1), the decomposition of tetragonal $\text{Li}_2\text{CaGeO}_4$ to Ca_2GeO_4 was observed according to the reaction (1):



The decomposition temperature decreases from 1125 °C to 1000 °C with increasing the x value. According to B. Monnay et al. [22], the synthesis of $\text{Li}_2\text{CaGeO}_4$ at 1100–1300 °C results in orthorhombic $\text{Li}_2\text{CaGeO}_4$. These data have not been confirmed by other researchers and the present study shows that pure $\text{Li}_2\text{CaGeO}_4$ exists only in the tetragonal form and melts incongruently at 980 °C.

In the range of x values from 0.65 to 0.98 and temperatures from 1000 to 920 °C (between lines a and b in Fig. 1), an orthorhombic solid solution $\text{Li}_{2+2x}\text{Ca}_{1-x}\text{GeO}_4$ and liquid are present, and in the range of values of x from 0.98 to 1.0 and temperatures up to 920 °C Li_4GeO_4 and liquid exist.

Below the described areas of partial melting (decomposition) the areas of solid state phases consist (under line b of the diagram). In a wide concentration and temperature range, at values of x from 0 to 0.78 and temperatures from 980 to 700 °C (between lines b, d and e in Fig. 1), a two-phase region of tetragonal $\text{Li}_2\text{CaGeO}_4$ and orthorhombic solid solution $\text{Li}_{2+2x}\text{Ca}_{1-x}\text{GeO}_4$ exists. X-ray diffractograms of part of the studied compositions are presented in Fig. 2.

According to the diagram rules the value of x in the $\text{Li}_{2+2x}\text{Ca}_{1-x}\text{GeO}_4$ solid solution phase does not have to depend on x in the initial composition and is constant for a given temperature. The value of x in the $\text{Li}_{2+2x}\text{Ca}_{1-x}\text{GeO}_4$ solid solution only slightly changes from 0.65 to 0.78 with decreasing the temperature (line d in Fig. 1). As should be expected, with increasing the x value into the initial composition, the amount of orthorhombic $\text{Li}_{2+2x}\text{Ca}_{1-x}\text{GeO}_4$ solid solution progressively increases from 0 to 100% while the amount of pure $\text{Li}_2\text{CaGeO}_4$ decreases from 100 to 0. It should be noted that the calculated weight ratios between the two phases based on the obtained diffractograms strictly follow the lever rule. For example, according to the lever rule, the weight ratio between the tetragonal $\text{Li}_2\text{CaGeO}_4$ and the orthorhombic $\text{Li}_{2+2x}\text{Ca}_{1-x}\text{GeO}_4$ solid solution should be 75/25 wt % and the calculated ratio according to the diffractogram is 78/22 wt%. For point 6–7 the values are 25/75 and 28/72, and for point 7–7 the values are 13/87 and 15/85, respectively. As can be seen, the ratio is in agreement with the lever rule with deviations of 3%. The calculated values of the cell parameters for the two phases for points from 1 to 7 at 700 and 900 °C showed that the tetragonal $\text{Li}_2\text{CaGeO}_4$ has parameters $a = 5.140 \text{ \AA}$ and $b = 6.592 \text{ \AA}$, with deviations from the average values up to 0.03%, and the solid solution has parameters $a = 10.841 \text{ \AA}$, $b = 6.335 \text{ \AA}$ and $c = 5.193 \text{ \AA}$, with deviations from the average values up to 0.9%. These values do not change with changing in the x values in the starting mixture and show a weak tendency to decrease with decreasing the temperature. As summarized results for this region: 1. The chemical composition is constant for $\text{Li}_2\text{CaGeO}_4$ and with a small change of x values from 0.65 to 0.78 for the solid solution $\text{Li}_{2+2x}\text{Ca}_{1-x}\text{Ca}_1$.

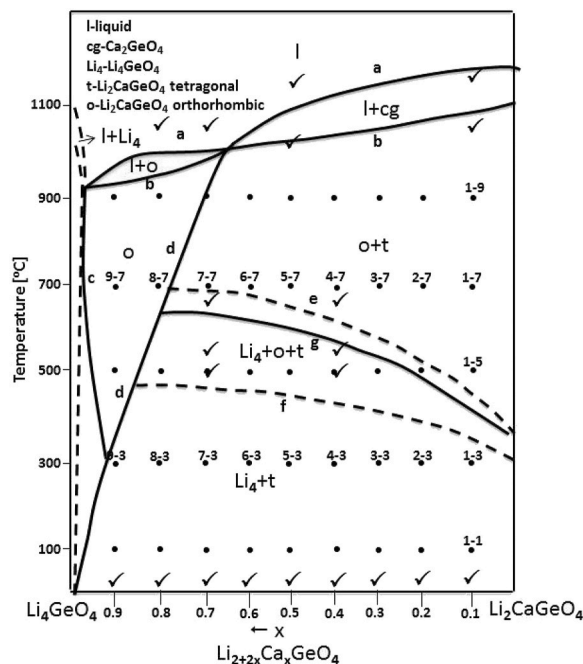


Fig. 1. Compositions and areas of crystallization in the $\text{Li}_4\text{GeO}_4\text{-Li}_2\text{CaGeO}_4$ system (1–9 corresponds to initial composition with $x = 0.1$ at 900 °C).

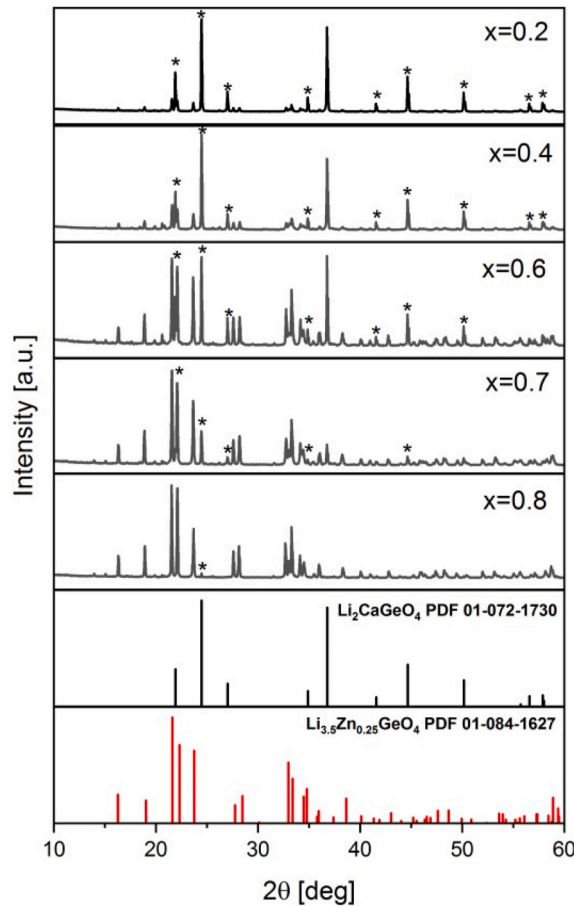


Fig. 2. X-ray diffractograms of part of the studied composition from two-phase region of tetragonal $\text{Li}_2\text{CaGeO}_4$ (marked by *) and orthorhombic solid solution $\text{Li}_{2+2x}\text{Ca}_{1-x}\text{GeO}_4$ at 700 °C.

$x\text{GeO}_4$ (line d) according to the synthesis temperature; 2. The weight ratio between the two phases progressively changes as x values changes in the starting solution in accordance to lever rule; 3. The obtained average values of the parameters for $\text{Li}_2\text{CaGeO}_4$ match well with the literature data [21]. There are no published data on the unit cell parameters of $\text{Li}_{2+2x}\text{Ca}_{1-x}\text{GeO}_4$ solid solutions.

Very important is the area closed with values of x from 0.65 to 0.98 and temperature from 1000 to 300 °C (between lines b, c and d in the Figure). This is a single-phase area of orthorhombic solid solution $\text{Li}_{2+2x}\text{Ca}_{1-x}\text{GeO}_4$. The area progressively narrows with lowering the temperature. At 900 °C it consists for x values from 0.65 to 0.98 and at 300 °C it exists only at $x = 0.92$. The obtained result is in good agreement with the data in the literature for 900 °C [23]. According to the diffractograms from this region, the unit cell parameters vary as follows: parameter a - from 10.840 Å to 10.839 Å, parameter b - from 6.332 Å to 6.327 Å and parameter c - from 5.195 Å to 5.189 Å. With increasing the x values (decreasing the content of Ca in the solution) and with decreasing the temperature, there is a tendency to decrease the volume of the unit cell. However, the differences do not exceed 0.7%.

The structure of the solid solution $\text{Li}_{2+2x}\text{Ca}_{1-x}\text{GeO}_4$ has not been reported in the literature. It was important to investigate this structure and compare it with the published structures for the analogous orthorhombic solid solutions $\text{Li}_{2+2x}\text{Zn}_{1-x}\text{GeO}_4$ and $\text{Li}_{2+2x}\text{Mg}_{1-x}\text{GeO}_4$ known under the name LISICON with high ionic conductivity [16–20]. Data of established structure of $\text{Li}_{2+2x}\text{Ca}_{1-x}\text{GeO}_4$ will be presented and discussed below.

Another broad two-phase region is located at x values from 0 to 0.98 and temperatures from 400 to 25 °C (below line f, in Fig. 1). In this area, orthorhombic Li_4GeO_4 and tetragonal $\text{Li}_2\text{CaGeO}_4$ crystallize. Some diffractograms from this region are presented in Fig. 3.

Similar to the already discussed two-phase region of $\text{Li}_2\text{CaGeO}_4$ and $\text{Li}_{2+2x}\text{Ca}_{1-x}\text{GeO}_4$, in this region the ratio between the two phases also changes progressively following the lever rule. The average values of the unit cell parameters of $\text{Li}_2\text{CaGeO}_4$ are $a = 5.138$ Å and $b = 6.591$ Å, and for Li_4GeO_4 $a = 7.760$ Å, $b = 6.049$ Å and $c = 7.362$ Å. The parameters are practically independent on the starting mixture composition and the temperature, and correspond to the literature data for the pure compounds (PDF-01-072-1730 and PDF-00-031-0719).

Surprisingly, in the range of x values from 0 to 0.88 and temperatures from 685 to 320 °C (between lines e and f in Fig. 1), the existence of the three main phases simultaneously (Li_4GeO_4 , $\text{Li}_2\text{CaGeO}_4$ and $\text{Li}_{2+2x}\text{Ca}_{1-x}\text{GeO}_4$) was found. This unusual result required

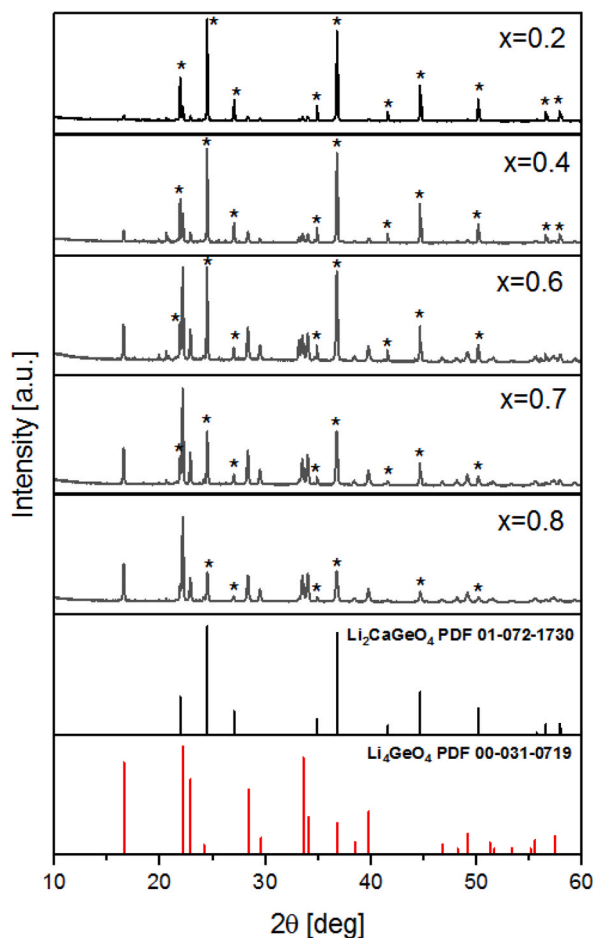


Fig. 3. X-ray diffractograms of part of the studied composition from two-phase region of tetragonal $\text{Li}_2\text{CaGeO}_4$ (marked by *) and orthorhombic Li_4GeO_4 at 300 °C.

further studies. For this, part of the samples synthesized at 300 °C was treated at 500, 600 and 650 °C for 120 h with 2 intermediate grindings. At the same regimes were treated samples synthesized at 900 °C. This additional studies with more intermediate grindings and extended synthesis time showed very slow reversible conversion of the two-phase system of Li_4GeO_4 and $\text{Li}_2\text{CaGeO}_4$ at low temperatures to a two-phase system of $\text{Li}_2\text{CaGeO}_4$ and $\text{Li}_{2+2x}\text{Ca}_{1-x}\text{GeO}_4$ at high temperatures. With an accuracy of ± 20 °C it was found that this transition occurs at temperatures from 400 to 650 °C depending on the x value. So line g in Fig. 1 is the boundary between the two two-phase regions. The reversible transition between those two regions can be expressed by the general formula (2):



The studies show that the mentioned reversible transition is very slow in the both directions, i.e. there is a metastable three-phase region, the width of which depends on the time of treatment of the samples. This region was also investigated by DSC/TG analyzes of samples synthesized at 900 °C and cooled to room temperature. The heating rate was 5 °C/min in air. DSC data of these samples are presented in Fig. 4.

During heating an endothermic effect is observed at a temperature in the range of 710–731 °C and during cooling, an exothermic effect is observed at temperatures in the range of about 550 °C. So, the rapid heating (cooling) of the samples shows the discussed metastable region again (some unexplained small effect at about 300 °C appears too). It should be noted that the thermal effects are more pronounced when the value of x is higher, i.e. the amount of Li_4GeO_4 is larger. This result is completely logical, given the fact that the solid solution realized during the reaction (according to the diagram) is with x above 0.78 (line d in Fig. 1), which requires a large amount of Li_4GeO_4 and a small amount of $\text{Li}_2\text{CaGeO}_4$. Since during heating and cooling the change in the sample mass is insignificant (within 0.5–0.8 mass %) there are not TG data presented in Fig. 4.

Another feature of the studied system is the behavior of samples after a long stay in air at 25 °C. It turns out that the samples become heavy, accompanied by some swelling. A special study showed that the degree of weighting is within 4.8–11%, increasing with the increase the value of x, i.e. with increasing the amount of Li_4GeO_4 in the two-phase system. The time for reaching a constant weight is in the same dependence on x value, and with increasing the x it increases from 7 to 12 days. X-ray phase analysis of these samples

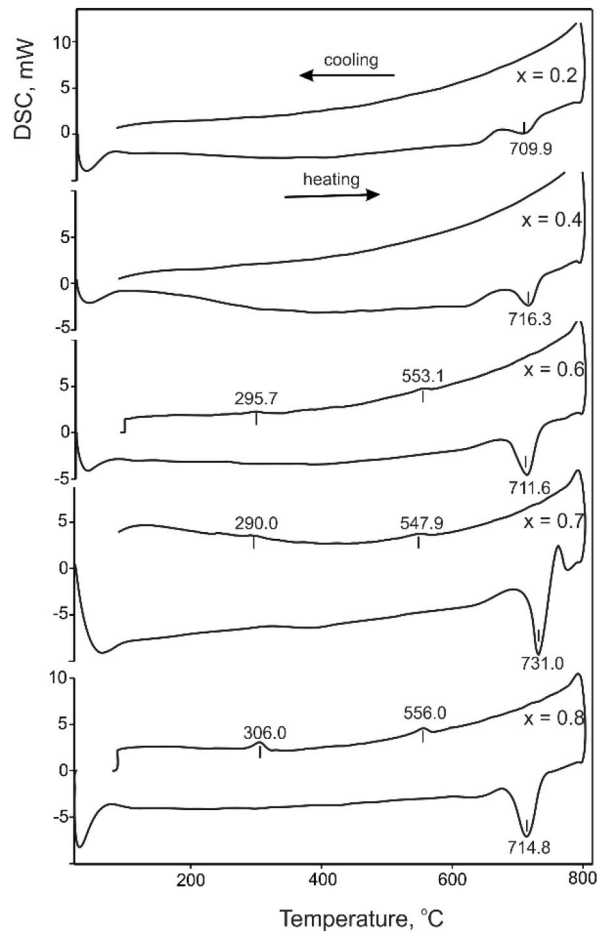


Fig. 4. DSC analyzes showing the transition between the two two-phase regions.

showed an appearance of small impurities of Li_2CO_3 and Li_2GeO_3 in the samples (Fig. 5).

Simultaneous DSC-TG-MS analyzes confirm this result. During heating of the samples a mass loss was established adequate to the already established weighting after long stay at 25 °C in air (Fig. 6). This reduction is higher when the x is higher (Fig. 6b). The heating is accompanied with an evolving of H_2O ($m/z = 18$) and CO_2 ($m/z = 44$). So, we are talking about a reaction of Li_4GeO_4 with CO_2 from the air and a transformation of Li_4GeO_4 to Li_2GeO_3 by the reaction (3):



This behavior of the system $\text{Li}_4\text{GeO}_4\text{-Li}_2\text{CaGeO}_4$ is very similar to that described in the literature for the systems $\text{Li}_4\text{GeO}_4\text{-Li}_2\text{ZnGeO}_4$ and $\text{Li}_4\text{GeO}_4\text{-Li}_2\text{MgGeO}_4$. Although $\text{Li}_4\text{GeO}_4\text{-Li}_2\text{ZnGeO}_4$ has not been studied below 300 °C, the sharp decrease in the ionic conductivity of solid solutions $\text{Li}_{2+2x}\text{Zn}_{1-x}\text{GeO}_4$ over time, according to the authors, is due to instability of the solid solution and its transformation to Li_2CO_3 and Li_2GeO_3 or other substructural modifications of the orthorhombic solid solution [17].

The final form of the diagram $\text{Li}_4\text{GeO}_4\text{-Li}_2\text{CaGeO}_4$ is presented in Fig. 7.

The comparison of the established phase equilibria with those in the $\text{Li}_4\text{GeO}_4\text{-Li}_2\text{ZnGeO}_4$ and $\text{Li}_4\text{GeO}_4\text{-Li}_2\text{MgGeO}_4$ systems shows several features of the $\text{Li}_4\text{GeO}_4\text{-Li}_2\text{CaGeO}_4$ system:

1. The presence of a much wider two-phase zone with tetragonal $\text{Li}_2\text{CaGeO}_4$ and orthorhombic $\text{Li}_{2+2x}\text{Ca}_{1-x}\text{GeO}_4$ solid solution at high temperatures.
2. Presence of a two-phase zone with tetragonal $\text{Li}_2\text{CaGeO}_4$ and orthorhombic Li_4GeO_4 .
3. At the expense of these two two-phase regions, the single-phase region of a solid solution is significantly narrower than that of solid solutions with Zn or Mg.

The obtained results seem to be explained by the fact that $\text{Li}_2\text{ZnGeO}_4$ and $\text{Li}_2\text{MgGeO}_4$ are orthorhombic at high temperatures and their interaction with the orthorhombic Li_4GeO_4 to obtain orthorhombic solid solution $\text{Li}_{2+2x}\text{Zn}_{1-x}\text{GeO}_4$ or $\text{Li}_{2+2x}\text{Mg}_{1-x}\text{GeO}_4$ is relieved. As it was established, pure $\text{Li}_2\text{CaGeO}_4$ has only tetragonal modification. An additional explanation is the fact that the ionic radius of

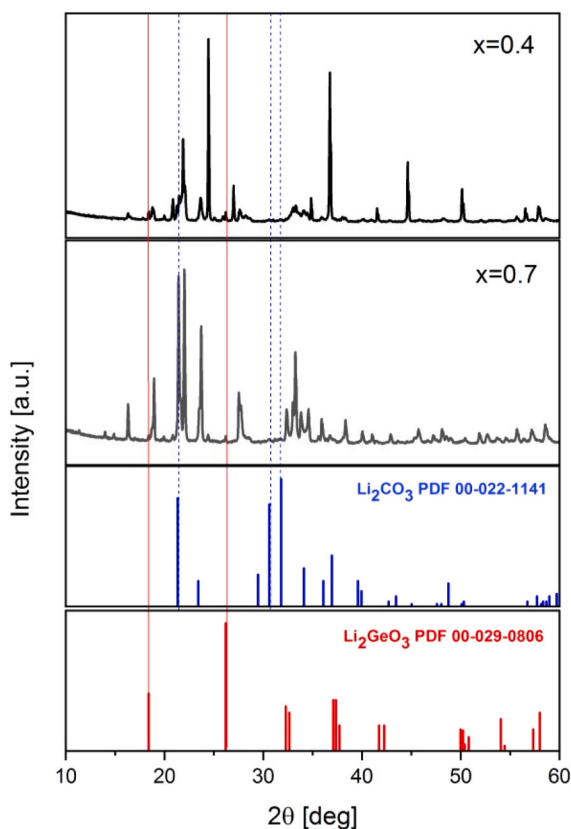


Fig. 5. X-ray diffractograms of part of the studied composition synthesized at 900 °C after long stay at 25 °C.

Ca^{2+} , unlike those of Zn^{2+} and Mg^{2+} , is too different from the ionic radius of Li^{1+} , which undoubtedly makes mutual substitution difficult.

The latter is an additional reason to investigate the structure of the $\text{Li}_{2+2x}\text{Ca}_{1-x}\text{GeO}_4$ solid solution and compare it with the structure of the other two solutions discussed.

The crystal structure of $\text{Li}_{3,62}\text{Ca}_{0,18}\text{GeO}_4$ is presented in Fig. 8, compared with that of $\text{Li}_{3,5}\text{Zn}_{0,25}\text{GeO}_4$ [19]. Both solid solutions crystallize in the orthorhombic space group $Pnma$ and have similar unit cell parameters ($a = 10.827 \text{ \AA}$, $b = 6.320 \text{ \AA}$, $c = 5.203 \text{ \AA}$ and $a = 10.885 \text{ \AA}$, $b = 6.268 \text{ \AA}$, $c = 5.155 \text{ \AA}$ for the Ca and Zn containing compounds respectively). The oxygen atoms of both compounds are arranged in a hexagonal close packing that includes tetrahedral and octahedral spaces. In $\text{Li}_{3,5}\text{Zn}_{0,25}\text{GeO}_4$ the tetrahedral positions are occupied by Ge, Zn and Li cations to form a tetrahedral framework with the composition $[\text{Li}_{2,75}\text{Zn}_{0,25}\text{GeO}_4]$. The excess of Li atoms are placed in the octahedral spaces, they are loosely bound to the framework. This location predetermine high ionic conductivity of the compound. In the case of $\text{Li}_{3,62}\text{Ca}_{0,18}\text{GeO}_4$, the tetrahedral spaces are occupied by Li and Ge atoms to form $[\text{Li}_{2,5}\text{GeO}_4]$ tetrahedral framework, while the excess of Li and Ca atoms are placed in the octahedral positions. Thus the Ca atoms hinder the mobility of the Li atoms. This explains the lower ionic conductivity of the $\text{Li}_{2+2x}\text{Ca}_{1-x}\text{GeO}_4$ solid solutions [23]. Due to the noted difference in the local environment of the ions, differences in other properties of the two solid solutions are expected (excitation, emission spectra and so on). The occupancy of Li and Ca atomic positions in the studied structures are presented in Table 1. Most important data collection and refinement parameters for the studied sample are presented in Table 2. Information about the additional structural data is available in the Cambridge Structural Database: CSD2299469.

4. Conclusion

Li_4GeO_4 - $\text{Li}_2\text{CaGeO}_4$ system by solid-phase syntheses of various compositions from pure Li_4GeO_4 to pure $\text{Li}_2\text{CaGeO}_4$ and from 25 to 1125 °C was investigated. The data obtained showed different phase regions: 1. wide temperature and concentration two-phase region of orthorhombic solid solution $\text{Li}_{2+2x}\text{Ca}_{1-x}\text{GeO}_4$ and tetragonal $\text{Li}_2\text{CaGeO}_4$ at temperatures from 400 °C up to 1125 °C and values of x from 0 to 0.8; 2. wide two-phase region of orthorhombic Li_4GeO_4 and $\text{Li}_2\text{CaGeO}_4$ at temperatures below 400 °C in the entire concentration range (x from 0 to 1.0); 3. narrow single-phase region of solid solution $\text{Li}_{2+2x}\text{Ca}_{1-x}\text{GeO}_4$ existing from 1000 °C to 300 °C and x values from 0.65 to 0.98. Compared the Li_4GeO_4 - $\text{Li}_2\text{CaGeO}_4$ system with Li_4GeO_4 - $\text{Li}_2\text{ZnGeO}_4$ and Li_4GeO_4 - $\text{Li}_2\text{MgGeO}_4$, the single-phase region with Ca is significantly richer in Li_4GeO_4 and significantly narrower. This difference could be explained by the lack of orthorhombic modification of $\text{Li}_2\text{CaGeO}_4$, and facilitates the interaction with orthorhombic Li_4GeO_4 , and by the large difference in the

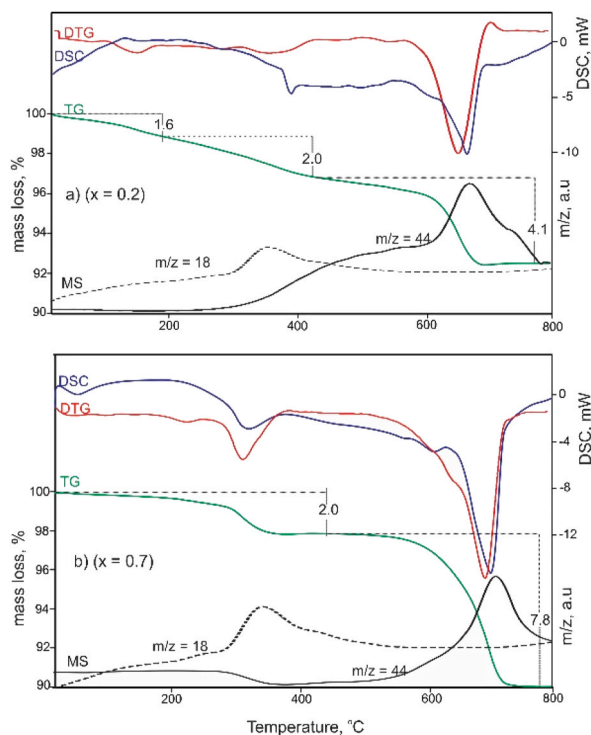


Fig. 6. DSC-TG-MS data of part of the studied composition synthesized at 900 °C after long stay at 25 °C: a) $x = 0.2$; b) $x = 0.7$.

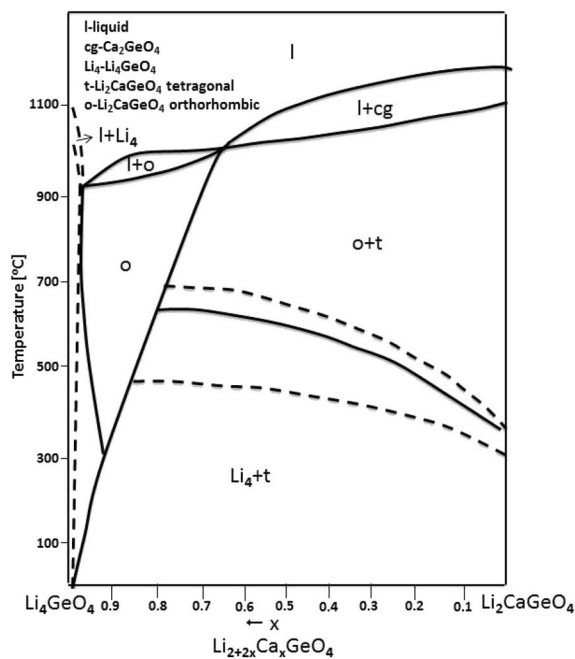


Fig. 7. Phase diagram $\text{Li}_4\text{GeO}_4 - \text{Li}_2\text{CaGeO}_4$.

ionic radii of Ca^{2+} and Li^{1+} , making mutual substitution difficult.

Another feature of the studied system is the behavior of samples after a long stay in air at 25 °C. X-ray phase analysis of the samples showed an appearance of small impurities of Li_2CO_3 and Li_2GeO_3 . Simultaneous DSC-TG-MS analyzes confirm this result. So, we are talking about a reaction of Li_4GeO_4 with CO_2 from the air and a transformation of Li_4GeO_4 to Li_2GeO_3 by the reaction. This behavior of

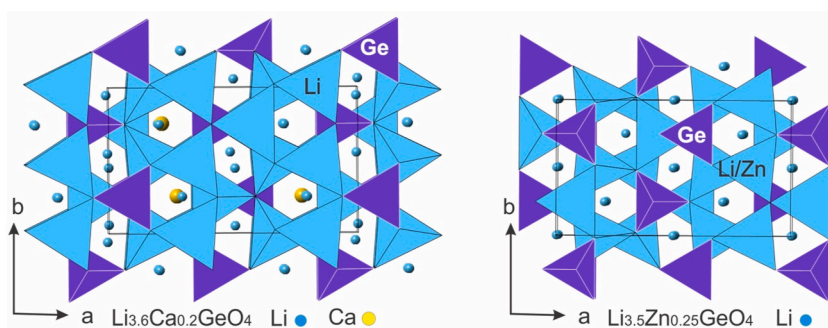


Fig. 8. Crystal structure of $\text{Li}_{3.62}\text{Ca}_{0.18}\text{GeO}_4$ compared with that of $\text{Li}_{3.5}\text{Zn}_{0.25}\text{GeO}_4$.

Table 1

The occupancy of Li and Ca atomic positions in $\text{Li}_{3.62}\text{Ca}_{0.18}\text{GeO}_4$ and Li and Zn atomic positions in $\text{Li}_{3.5}\text{Zn}_{0.25}\text{GeO}_4$ solid solutions.

$\text{Li}_{3.62}\text{Ca}_{0.18}\text{GeO}_4$			$\text{Li}_{3.5}\text{Zn}_{0.25}\text{GeO}_4$			
Atom	Fractional coordinates	Site occupancy	Atom	Fractional coordinates	Site occupancy	Coordination number
Li1	0.662 0.007 0.832	78%	Li1/Zn1	0.43 0.750 0.186	Li 92%, Zn 8%	4
Li2	0.421 0.250 0.833	78%	Li2/Zn2	0.16 0.989 0.358	Li 92%, Zn 8%	4
Li3	0.670	22%	Li3	0.169 0.043 0.184	24%	4
	0.069 0.605					
Li4	0.508 0.053 0.920	22%	Li4	0.208 0.250 0.945	34%	6
Li5	0.703 0.750 0.481	40%	Li5	0.000 0.000 0.500	6%	6
Ca	0.719 0.750 0.427	18%				6

Table 2

Most important data collection and refinement parameters for the studied sample.

Compound	$\text{Li}_{2+2-x}\text{Ca}_{1-x}\text{GeO}_4$
Chemical formula	$\text{Li}_{3.6}\text{Ca}_{0.2}\text{GeO}_4$
Formula weight	168.39
Temperature/K	277.0
Crystal color	colorless
Crystal system	Orthorhombic
Space group	$P n m a$
a/Å	10.8272 (5)
b/Å	6.3203 (3)
c/Å	5.2033 (2)
$\alpha = \beta = \gamma/\%$	90
Volume/Å ³	356.07 (3)
Z	4
ρ_{calc} (mg/cm ³)	3.141
μ/mm^{-1}	8.692
F (000)	313
Crystal size/mm ³	0.05 × 0.05 × 0.05
Radiation, λ [Å]	MoKα, λ = 0.71073
θ range for data collection/°	7.528 to 69.966
Limiting indices	-17 ≤ h ≤ 17, -10 ≤ k ≤ 10, -7 ≤ l ≤ 8
Reflections collected/unique	6157/845 [R (int) = 0.0315]
Refinement method	Full-matrix least-squares on F ²
Data/restraints/parameters	845/0/67
Goodness-of-fit on F ²	1.145
Final R indexes [I ≥ 2σ (I)]	RI = 0.0233, wR2 = 0.0452
Final R indexes [all data]	RI = 0.0277, wR2 = 0.0463
Largest diff. peak/hole/e Å ⁻³	0.57/-0.88

the system Li_4GeO_4 – $\text{Li}_2\text{CaGeO}_4$ is very similar to that described in the literature for the systems Li_4GeO_4 – $\text{Li}_2\text{ZnGeO}_4$ and Li_4GeO_4 – $\text{Li}_2\text{MgGeO}_4$. Although Li_4GeO_4 – $\text{Li}_2\text{ZnGeO}_4$ has not been studied below 300 °C, the sharp decrease in the ionic conductivity of solid solutions $\text{Li}_{2+2x}\text{Zn}_{1-x}\text{GeO}_4$ over time, according to the authors, is due to instability of the solid solution and its transformation to Li_2CO_3 and Li_2GeO_3 or other substructural modifications of the orthorhombic solid solution.

The studied structure of the $\text{Li}_{2+2x}\text{Ca}_{1-x}\text{GeO}_4$ solid solution shows that, despite the analogy with $\text{Li}_{2+x}\text{Zn}_{1-x}\text{GeO}_4$ and $\text{Li}_{2+x}\text{Mg}_{1-x}\text{GeO}_4$ structure, the local environments of the metal ions are very different. This difference implies different properties of solid

solutions. For example the too low ionic conductivity of $\text{Li}_{2+x}\text{Ca}_{1-x}\text{GeO}_4$ compared to that of the other two solutions cited in the literature can be explained by this difference.

Data availability statement

Information about the additional structural data is available in the Cambridge Structural Database: CSD2299469.

CRediT authorship contribution statement

V. Nikolov: Writing – original draft, Methodology, Data curation, Conceptualization. **R. Nikolova:** Software, Data curation. **N. Petrova:** Software, Data curation. **P. Tzvetkov:** Software, Data curation. **I. Koseva:** Writing – review & editing, Visualization, Data curation.

Declaration of competing interest

The authors declare that they have no known competing financial interests or personal relationships that could have appeared to influence the work reported in this paper.

Acknowledgments

The research is financial supported by the National Science Fund of Bulgaria (Contract No. KP-06-H79/2). R.N. acknowledge project CoE “National Center of Mechatronics and Clean Technologies”, BG05M2OP001-1.001-0008 for single crystal structural analyses.

References

- [1] J. Chen, Y. Tang, C. Yin, M. Yu, H. Xiang, C. Li, X. Hung, L. Fang, Structure, microwave dielectric performance, and infrared reflectivity spectrum of olivine-type $\text{Mg}_2\text{Ge}_{0.98}\text{O}_4$ ceramic, *J. Am. Ceram. Soc.* 103 (2020) 1789–1797, <https://doi.org/10.1111/jace.16855>.
- [2] S. Wu, Q. Ma, Synthesis, characterization and microwave dielectric properties of Zn_2GeO_4 ceramics, *J. Alloys Compd.* 567 (2013) 40–46, <https://doi.org/10.1016/j.jallcom.2013.03.052>.
- [3] H. Yang, J. Shi, M. Gong, H. Liang, The UV and VUV luminescence properties of the phosphor $\text{Mg}_2\text{GeO}_4:\text{Tb}^{3+}$, *Mater. Lett.* 64 (2010) 1034–1036, <https://doi.org/10.1016/j.matlet.2010.02.001>.
- [4] H.M. Yang, Z. Wang, M.L. Gong, H. Liang, Luminescence properties of a novel red emitting phosphor, $\text{Mg}_2\text{GeO}_4:\text{Sm}^{3+}$, *J. Alloys Compd.* 488 (2009) 331–333, <https://doi.org/10.1016/j.jallcom.2009.08.123>.
- [5] C. Li, H. Xiang, M. Xu, Y. Tang, L. Fang, Li_2AGeO_4 (A= Zn, Mg): two novel low-permittivity microwave dielectric ceramics with olivine structure, *J. Eur. Ceram. Soc.* 38 (2018) 1524–1528, <https://doi.org/10.1016/j.jeurceramsoc.2017.12.038>.
- [6] J.I. Viegas, R.L. Moreira, A. Dias, Optical-vibration properties of $\text{Li}_2\text{ZnGeO}_4$ dielectric ceramics, *Vibr. Spectrosc.* 110 (2020) 103130, <https://doi.org/10.1016/j.vibspec.2020.103130>.
- [7] Y. Jin, Y. Hu, Different luminescent behaviors between photoluminescence and persistent luminescence in Tb^{3+} doped $\text{Li}_2\text{CaGeO}_4$ phosphors, *Mater. Res. Bull.* 61 (2015) 16–21, <https://doi.org/10.1016/j.materresbull.2014.09.085>.
- [8] I.V. Berezovskaya, N.P. Efryushina, I.I. Seifullina, E.E. Martsinko, B.I. Zadneprovski, G.B. Stryganyuk, A.S. Voloshinovskii, S.M. Levshov, V.P. Dotsenko, Luminescence properties of Eu^{2+} and Ce^{3+} ions in calcium lithio-germanate $\text{Li}_2\text{CaGeO}_4$, *Ceram. Int.* 39 (2013) 6835–6840, <https://doi.org/10.1016/j.ceramint.2013.02.015>.
- [9] R. Cao, D. Ceng, X. Yu, S. Guo, Y. Wen, G. Zheng, Synthesis and luminescence properties of novel deep red emitting phosphors $\text{Li}_2\text{MgGeO}_4:\text{Mn}^{4+}$, *Funct. Mater. Lett.* 8 (2015) 1550046, <https://doi.org/10.1142/S1793604715500460>.
- [10] N. Bednarska-Adam, M. Kuwik, E. Pietrasik, W.A. Pisarski, T. Goryczka, B. Macalik, J. Pisarska, Synthesis and characterization of $\text{Li}_2\text{MgGeO}_4:\text{Ho}^{3+}$, *Mater* 15 (2022) 5263, <https://doi.org/10.3390/ma15155263>.
- [11] Y. Jin, Y. Hu, H. Duan, L. Chen, X. Wang, The long persistent luminescence properties of phosphors: $\text{Li}_2\text{ZnGeO}_4$ and $\text{Li}_2\text{ZnGeO}_4:\text{Mn}^{2+}$, *RSC Adv.* 4 (2014) 11360–11366, <https://doi.org/10.1039/C3RA47760F>.
- [12] C. Li, J. Xu, W. Liu, D. Zheng, S. Zhang, Y. Zhang, H. Lin, N. Liu, J. Liu, F. Zeng, Synthesis and characterization of Cr^{4+} -doped Ca_2GeO_4 tunable crystal, *J. Alloys Compd.* 636 (2015) 211–215, <https://doi.org/10.1016/j.jallcom.2015.02.121>.
- [13] D. Wang, X. Zhang, X. Wang, Z. Leng, Q. Yang, W. Ji, H. Lin, F. Zeng, C. Li, Z. Su, Investigation of the structural and luminescent properties and the chromium ion valence of $\text{Li}_2\text{CaGeO}_4$ crystals doped with Cr^{4+} ions, *Cryst* 10 (2020) 1019, <https://doi.org/10.3390/cryst10111019>.
- [14] C. Jousseau, A. Kahn-Harari, J. Derouet, D. Vivien, Spectroscopic characterization of chromium in $\text{Li}_2\text{MgSiO}_4$ single crystals, in: *Advanced Solid State Lasers*, Optica Publishing Group, 2002, p. TuB12, <https://doi.org/10.1364/ASSL.2002.TuB12>, February.
- [15] C. Anino, J. Théry, D. Vivien, $(\text{CrO}_4)^{4-}:\text{Li}_2\text{MgSiO}_4$, a near IR broad-band emitting material with very long fluorescence lifetime, in: *Advanced Solid State Lasers*, Optica Publishing Group, 1997, p. SC6, <https://doi.org/10.1364/ASSL.1997.SC6>, January.
- [16] H.P. Hong, Crystal structure and ionic conductivity of $\text{Li}_{1.4}\text{Zn}(\text{GeO}_4)_4$ and other new Li^+ superionic conductors, *Mater. Res. Bull.* 13 (1978) 117–124, [https://doi.org/10.1016/0025-5408\(78\)90075-2](https://doi.org/10.1016/0025-5408(78)90075-2).
- [17] P.G. Bruce, A.R. West, Phase diagram of the LISICON, solid electrolyte system, $\text{Li}_4\text{GeO}_4\text{-Zn}_2\text{GeO}_4$, *Mater. Res. Bull.* 15 (1980) 379–385, [https://doi.org/10.1016/0025-5408\(80\)90182-8](https://doi.org/10.1016/0025-5408(80)90182-8).
- [18] E. Plattner, H. Völlenkle, Die Kristallstruktur der Verbindung $\text{Li}_3\text{Zn}_{0.5}\text{GeO}_4$, *Monatshfte für Chemie/Chemical Monthly* 110 (1979) 693–698, <https://doi.org/10.1007/BF00938373>.
- [19] I. Abrahams, P.G. Bruce, A.R. West, W.I.F. David, Structure determination of LISICON solid solutions by powder neutron diffraction, *J. Solid State Chem.* 75 (1988) 390–396, [https://doi.org/10.1016/0022-4596\(88\)90179-X](https://doi.org/10.1016/0022-4596(88)90179-X).
- [20] I. Abrahams, P.G. Bruce, W.I.F. David, A.R. West, A re-examination of the LISICON structure using high-resolution powder neutron diffraction: evidence for defect clustering, *Acta Crystallogr. B* 45 (1989) 457–462, <https://doi.org/10.1107/S0108768189006245>.
- [21] J.A. Gard, A.R. West, Preparation and crystal structure of $\text{Li}_2\text{CaSiO}_4$ and isostructural $\text{Li}_2\text{CaGeO}_4$, *J. Solid State Chem.* 7 (1973) 422–427, [https://doi.org/10.1016/0022-4596\(73\)90171-0](https://doi.org/10.1016/0022-4596(73)90171-0).
- [22] B. Monnaye, C. Garrault, G. Perez, R. Bouaziz, Sur une famille d'orthogermanates doubles de lithium $\text{Li}_2\text{M(II)GeO}_4$ avec $\text{M(II)} = \text{Mg, Ca, Fe, Co, Ni, Zn, Cd}$. Structure cristalline de $\text{Li}_2\text{MgGeO}_4$, *C. R. Acad. Sci. [Paris] C* 278 (1974) 251–253.

- [23] A.R. Rodger, J. Kuwano, A.R. West, Li⁺ ion conducting γ solid solutions in the systems Li₄XO₄-Li₃YO₄: X= Si, Ge, Ti; Y= P, as, V; Li₄XO₄-LiZO₂: Z= Al, Ga, Cr and Li₄GeO₄-Li₂CaGeO₄, Solid State Ionics 15 (1985) 185–198, [https://doi.org/10.1016/0167-2738\(85\)90002-5](https://doi.org/10.1016/0167-2738(85)90002-5).
- [24] R.O. Diffraction, CrysAlis Pro, Rigaku Corporation, Tokyo, Japan, 2015.
- [25] G. Sheldrick, SHELXL-97, Program for Crystal-Structure Refinement, 1997.
- [26] G.M. Sheldrick, Shelxt - integrated space-group and crystal-structure determination, Acta Crystallogr A Found Adv 71 (2015) 3–8, <https://doi.org/10.1107/S2053273314026370>.